ChemComm

Accepted Manuscript

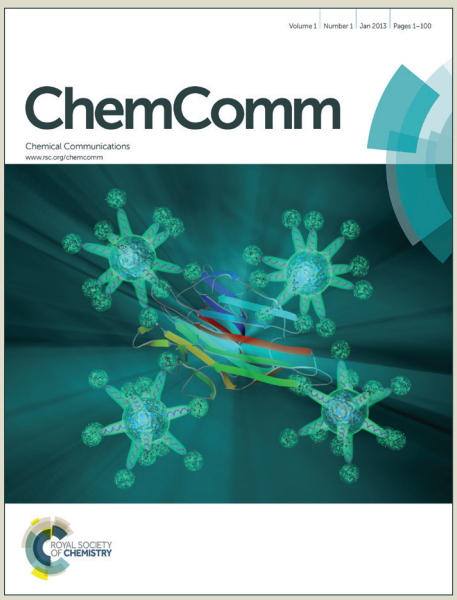

ROYAL SOCIETY OF CHEMISTRY

www.rsc.org/chemcomm

Journal Name

RSCPublishing

COMMUNICATION

A kinetically protected pyrene: molecular design, bright blue emission in the crystalline state and aromaticity relocation in its dicationic species

Cite this: DOI: 10.1039/x0xx00000x

Received 00th January 2012,
Accepted 00th January 2012

DOI: 10.1039/x0xx00000x

www.rsc.org/

Akinobu Matsumoto,[a] Mitsuharu Suzuki,[a] Daiki Kuzuhara,[a] Junpei Yuasa,[a] Tsuyoshi Kawai,[a] Naoki Aratani*[a] and Hiroko Yamada*[a,b]

Abstract: Sterically congested tetraarylpyrenes exhibited emission in both solution and the solid state. The monocationic species of pyrene 1 could be isolated because of the reasonably protected system. The aromaticity of 1 relocates from the biphenyl part to the naphthalene unit upon two-electron oxidation.

Pyrene derivatives are in general highly emissive and find many applications in optical sensors, nonlinear optics, and light emitting diodes.[1] We have recently succeeded in preparing blue-fluorescent pyrene-anthracene hybrid which was generated in-situ by photo-irradiation of its non-luminous diketone form in polymer matrix.[2] A well-known problem with pyrene systems is that their emission in the solid state is effectively quenched because of the formation of self-aggregation via π-π stacking.[3] A parent pyrene emission is pure blue to permit readily exploitation as an emissive material in organic light emitting diodes (OLEDs); however its tendency to form face-to-face dimers in the excited state constitutes a severe problem. Many research groups have attempted to enhance the emission of pyrene in the solid state by modifying its molecular structure.[4] Tetraphenylpyrene (**TPPy**, Scheme 1) is highly fluorescent (Φ ~ 0.9) in solution,[5] but the organic light-emitting field-effect transistor devices have been shown to exhibit electroluminescence with an external quantum efficiency of only 0.5%.[6] Sterically congested mesityl substituents can prevent undesirable face-to-face π-stacking, so that self-quenching is impeded to permit efficient emission in the solid state.[7] In reverse, aggregation-induced emission (AIE) is one of the most elegant strategies for making solid-state pyrene emissive.[8] The molecules are non-emissive when dissolved in a good solvent but become highly luminescent when aggregated in a poor solvent. In solution, the active rotations of the Ph groups at the periphery non-radiatively deactivate its excitons. In the aggregate state, however, the rotational restriction effectively blocks the non-radiative channel and hence makes pyrene highly emissive.[8]

Here we report synthesis and photophysical properties of a series of peripherally substituted pyrene derivatives, 1,3,6,8-(tetranaphthalen-1-yl)pyrene (**1**), 1,3,6,8-(tetraanthracen-9-yl)pyrene (**2**), and 4,5,9,10-(tetranaphthalen-1-yl)pyrene (**3**) to investigate the effect of bulky substituents at the periphery of the pyrene on their photophysical and electrochemical properties. We are intrigued to learn how its photoluminescence in solution and the solid state depends on the peripheral attachment. In addition to the facile synthetic accessibility by Suzuki–Miyaura cross-coupling, the bulky aryl rings were a priori anticipated to contribute to the improvement of the redox stability of pyrene derivatives.

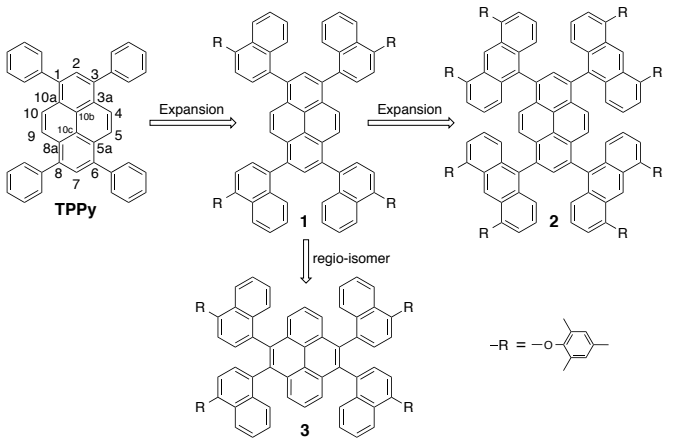

Scheme 1. Sterically hindered pyrene derivatives.

Synthesis of tetraarylpyrene **1**, **2** and **3** is shown in Scheme 2. Borylation of 1,3,6,8-tetrabromopyrene (**4**) by nickel catalyzed coupling reaction[9] gave 1,3,6,8-tetraborylpyrene **5**[10] as a crystalline solid in 74% yield. This compound serves as a versatile platform in the synthesis of tetrasubstituted pyrenes. Slow vapour diffusion of toluene into a chloroform solution of **5** afforded crystals suitable for X-ray diffraction analysis (Fig. S19).† Coupling of **5** with 1-bromo-4-mesityloxynaphthalene (**6**) furnished 1,3,6,8-tetrakis(4-mesityloxy-naphthyl)pyrene (**1**) in 32% yield. The structure of **1** was characterized

by mass spectroscopy and ^{1}H and ^{13}C NMR spectroscopy (ESI).† Compound **2** was obtained from the coupling reaction of **5** with the corresponding bromoanthracene **7**[11] in 40% yield. Similarly, compound **3** was obtained from the coupling reaction of **8**[12] with **9** in 18% yield.

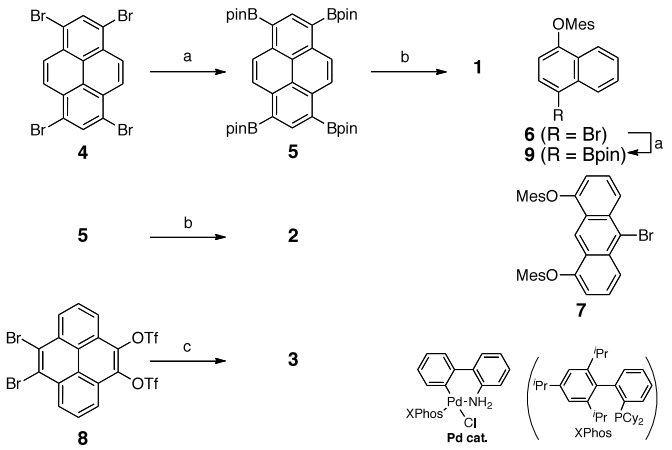

Scheme 2. Synthesis of naphthalene- and anthracene-linked pyrene derivatives. Reaction conditions: a) HBpin, $NiCl_2(dppp)$, b) **6**, K_3PO_4, Pd cat. and c) **9**, K_3PO_4, Pd cat. Bpin = 3,3,4,4-tetramethyl-1,3,2-dioxaborolanyl, Mes = mesityl.

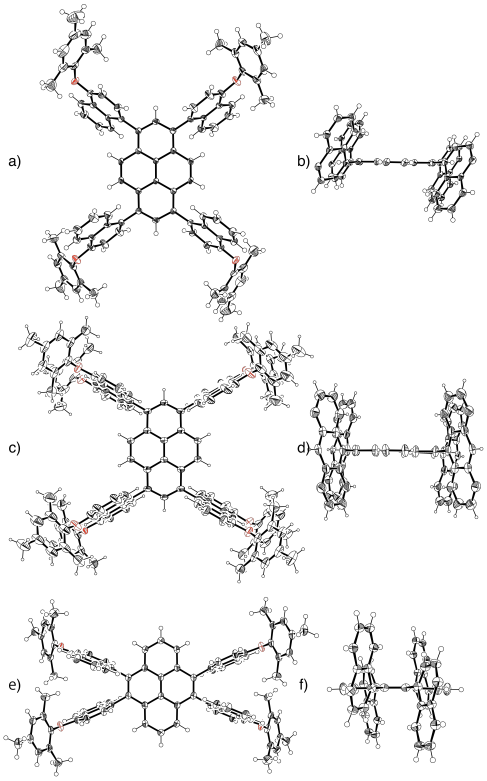

Fig. 1. Crystal structures of **1**, **2** and **3**: a) top view and b) side view of **1**, c) top view and d) side view of **2**, and e) top view and f) side view of **3**. Solvent molecules and mesityloxy groups in the side views are omitted for clarity. Thermal ellipsoids represent 50% for **1** and **3**, and 20% for **2**.

The structures of **1**, **2** and **3** were unambiguously confirmed by single-crystal X-ray diffraction analysis (Fig. 1).†[13] Each pyrene core unit is perfectly planar and does not form face-to-face stacking owing to the peripheral aryl groups. The naphthyl units in **1** are considerably tilted (64°) from the orthogonal arrangement. The anthryl units in **2** and naphthyl units in **3** are almost perpendicular to the core pyrene (83° and 84°, respectively) owing to the steric hinderance.

UV-vis absorption and fluorescence spectra of **1**, **2** and **3** in toluene along with pyrene are shown in Fig. 2a. Compared to the parent pyrene (λ_{max} = 337 nm), **1** exhibits distinctly red-shifted and broader absorption (λ_{max} = 372 nm), suggesting the electronic communication between the pyrene and naphthyl units. It is found that the peripheral anthracene units for **2** have absorption occurring at longer wavelength than the core pyrene. The vibrational structure of fluorescence of **3** may indicate its electronically unperturbed pyrene nature. The fluorescence quantum yields of **1** and **3** in toluene are 16 and 9%, respectively, thus the position of substituents affects the fluorescence properties. The fluorescence of **2** comes from anthracene units (Φ = 65%). To understand their electronic features, MO calculations of the model compounds **1'**, **2'** and **3'** (mesityl groups were replaced by methyl groups) were performed at the B3LYP/6-31G(d) level using the Gaussian 09 package[14] (Fig. S16). At a glance, the HOMOs of **1'** and **3'** are localized on the pyrene unit, while that of **2'** is localized on the anthracene units. The difference of the intramolecular interaction in **1** and **3** was also confirmed by cyclic voltammetry (CV). The CV of **1** in CH_2Cl_2 displayed two reversible oxidation potentials at 0.63 and 0.81 V (versus Fc/Fc^+ ion couple, Fig. S12). On the other hand, that of **3** exhibits an oxidation potential at 0.80 V as a quasi-reversible wave.

To investigate their solid state properties, fluorescence spectra and fluorescence quantum yields of the single crystals of **1**, **2** and **3** have been measured (Fig. 2b). The peak fluorescence wavelengths of the crystalline state are at 469, 469 and 404 nm, which are longer than those observed in solution, thus indicating intermolecular interactions and packing effects of **1**-**3** within the crystalline state. The florescence quantum yield of **1** in the solid state (37%) is much higher than that in solution, thus **1** exhibits AIE effect.

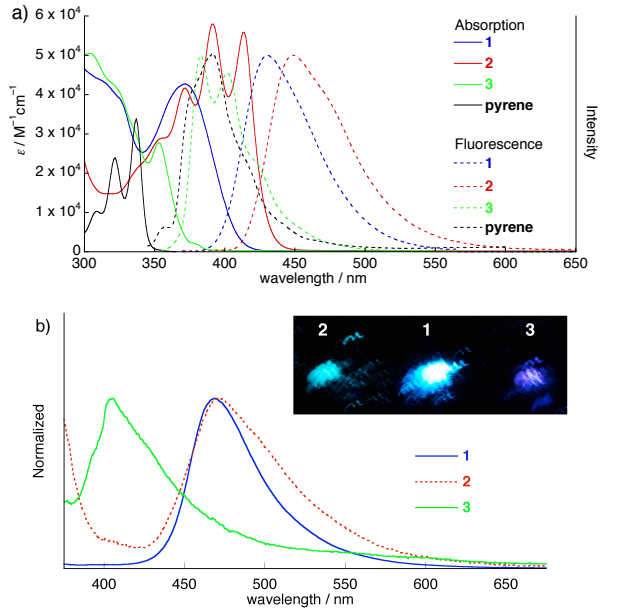

Fig. 2. a) UV-vis absorption and fluorescence spectra of **1**-**3** along with pyrene in toluene. b) Solid state fluorescence spectra of **1**-**3**. Inset: A photograph of crystals of **1**-**3** under irradiation with a hand-held UV lamp (365 nm).

The reversible oxidation found for **1** encouraged us to investigate the ability of **1** for the generation of cationic and dicationic species.[15] The oxidation of **1** was carried out with $SbCl_5$, which is known as a powerful oxidation agent. The UV-vis-NIR absorption spectra are depicted in Fig. 3. For **1**, the strong band at 372 nm incrementally disappeared, whereas new bands in the NIR region arose (major band at 1570 nm) after addition of 40 equivalents of $SbCl_5$. The formation of the radical cation was assumed, because an unpaired electron was clearly detected by ESR spectroscopy (Fig. S17). The stable cationic species was precipitated from the CH_2Cl_2 solution, to enable the isolation of $\mathbf{1}^{\bullet+}$ as an ionic salt. The absorption spectrum of this salt is practically the same as that of the electrochemically oxidized **1** at 0.8 V (Fig. S15). The half-life period of $\mathbf{1}^{\bullet+}$ upon exposure to air was measured to be more than 50 h, indicating the stable radical cation. Upon further addition of $SbCl_5$ (320 eq.), $\mathbf{1}^{\bullet+}$ was further oxidized to the formation of the dicationic species resulting in the appearance of NIR band at 1253 nm (Fig. 3a), and the disappearance of ESR signals. In order to check the aromaticity of the charged species, we performed NICS(0) calculations for **1**, $\mathbf{1}^{\bullet+}$ and $\mathbf{1}^{\bullet\bullet2+}$ by DFT method (B3LYP/6-31G(d)). By the electronic system rearrangement upon the oxidation, the bond lengths at C4-C5 and C9-C10 in **1** become longer and those at C3a-C4, C5-C5a, C8a-C9 and C10-C10a become shorter, being close to naphthalene. Eventually the aromaticity of the pyrene (larger negative NICS(0) value) relocates from the biphenyl part into the naphthalene unit upon the two-electron oxidation (Fig. 3b). This concept, to the best of our knowledge, is without precedent in the literature.

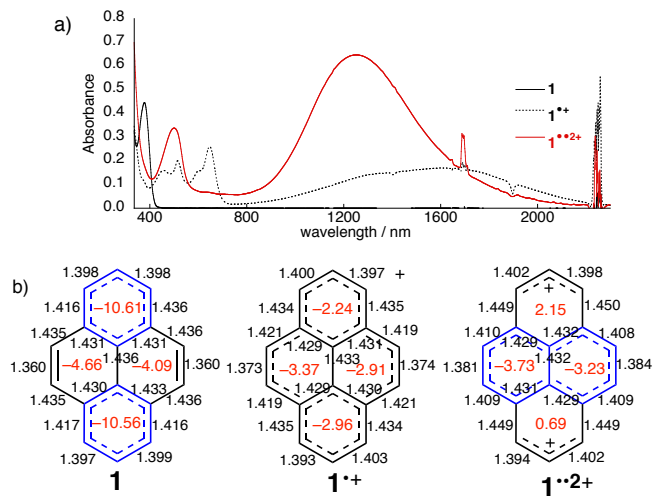

Figure 3. a) UV/Vis/NIR absorption spectra of **1**, $\mathbf{1}^{\bullet+}$ and $\mathbf{1}^{\bullet\bullet2+}$ formed under the oxidation with $SbCl_5$ in CH_2Cl_2 at room temperature. b) Bond lengths (in black) and NICS(0) values (in red) at the selected positions of **1**, $\mathbf{1}^{\bullet+}$ and $\mathbf{1}^{\bullet\bullet2+}$ based on the DFT calculations. Aromatic circuit is drawn in blue for guidance.

In conclusion, we report herein that the pyrenes functionalized by sterically hindered aryl groups do not undergo close π-stacking leading to solid-state emission properties that parallel those in the solution state. Sterically hindered pyrene **1** underwent two-electron oxidation with $SbCl_5$ to give the persistent pyrene dication. We will show that such molecular systems lend themselves to application as pure-blue emissive materials in OLEDs in near future.

This work was partly supported by Grants-in-Aid for Scientific Research (Nos. 25288092, 25620061, 26288038 and 25107519 'AnApple'), for Young Scientists (A) (No. 23685030), a research grant by The Murata Science Foundation, PRESTO program by JST, and the Green Photonics Project in NAIST supported by MEXT. We thank Mr. S. Katao, NAIST, for the X-ray diffraction analysis and Ms. Y. Nishikawa, NAIST, for the mass spectroscopy.

Notes and references

[a] Graduate School of Materials Science, Nara Institute of Science and Technology (NAIST), 8916-5 Takayama-cho, Ikoma 630-0192 Japan, E-mail: aratani@ms.naist.jp, hyamada@ms.naist.jp, Fax: +81-743-72-6042.
[b] CREST, Japan Science and Technology (JST) Agency, 4-1-8 Honcho, Kawaguchi, Saitama 332-0012, Japan.

† Electronic supplementary information (ESI) available: Supplementary figures, experimental procedures, spectroscopic and crystallographic data. CCDC-1001880 (**1**), 1001881 (**2**), 1001882 (**3**) and 1001883 (**5**). For ESI and crystallographic data in CIF see DOI: 10.1039/c000000x/

1 T. M. Figueira-Duarte and K. Müllen, *Chem. Rev*. 2011, **111**, 7260–7314.
2 T. Aotake, H. Tanimoto, H. Hotta, D. Kuzuhara, T. Okujima, H. Uno and H. Yamada, *Chem. Commun*. 2013, **49**, 3661–3663.
3 F. Würthner, C. Thalacker, S. Dieke and C. Tschierske, *Chem. Eur. J*. 2001, **7**, 2245–2253.
4 F. M. Winnik, *Chem. Rev*. 1993, **93**, 587; G. Venkataramana and S. Sankararaman, *Org. Lett*. 2006, **8**, 2739; V. de Halleux, J.-P.Calbert, P. Brocorens, J. Cornil, J.-P. Declercq, J. L. Bredas and Y. Geerts, *Adv. Funct. Mater*. 2004, **14**, 649; D. Rausch and C. Lambert, *Org. Lett*. 2006, **8**, 5037.
5 I. B. Berlman, *J. Phys. Chem*. 1970, **74**, 3085.
6 T. Oyamada, H. Uchiuzou, S. Akiyama, Y. Oku, N. Shimoji, K. Matsushige, H. Sasabe and C. Adachi, *J. Appl. Phys*. 2005, **98**, 074506.
7 J. N. Moorthy, P. Natarajan, P. Venkatakrishnan, D.-F. Huang and T. J. Chow, *Org. Lett*. 2007, **9**, 5215−5218.
8 Z. Zhao, S. Chen, J. W. Y. Lam, P. Lu, Y. Zhong, K. S. Wong, H. S. Kwok and B. Z. Tang, *Chem. Commun*. 2010, **46**, 2221–2223.
9 A. B. Morgan, J. L. Jurs and J. M. Tour, *J. Appl. Polym. Sci*. 2000, **76**, 1257–1268.
10 M. N. Eliseeva and L. T. Scott, *J. Am. Chem. Soc*. 2012, **134**, 15169–15172; B. A. G. Hammer, M. Baumgarten and K. Müllen, *Chem. Comm*. 2014, **50**, 2034–2036.
11 K. Naoda, H. Mori, N. Aratani, B. S. Lee, D. Kim and A. Osuka, *Angew. Chem. Int. Ed*. 2012, **51**, 9856–9859.
12 L. Zöphel, V. Enkelmann, R. Rieger and K. Müllen, *Org. Lett*. 2011, **13**, 4506–4509.
13 The contributions to the scattering arising from the presence of disordered solvents in the crystals of **2** and **3** were removed by use of the utility SQUEEZE in the PLATON software package.[16]
14 For the full citation, see the ESI.
15 K. K. Laali, P. E. Hansen, E. Gelerinter and J. J. Houser, *J. Org. Chem*. 1993, **58**, 4088–4095.
16 Squeeze-Platon: A. L. Spek, *PLATON, A Multipurpose Crystallographic Tool*, Utrecht, The Netherlands, 2005; P. van der Sluis and A. L. Spek, *Acta Crystallogr. Sect. A* 1990, **46**, 194–201.